Physics of Plasmas ARTICLE scitation.org/journal/php

Producing a magnetized low energy, high electron charge density state using a split cathode

Cite as: Phys. Plasmas **27**, 103102 (2020); doi: 10.1063/5.0022115
Submitted: 17 July 2020 · Accepted: 20 September 2020 ·
Published Online: 12 October 2020

J. G. Leopold,[1,a)] Ya. E. Krasik,[1] Y. P. Bliokh,[1] and E. Schamiloglu[2]

AFFILIATIONS

[1]Physics Department, Technion, Israel Institute of Technology, Haifa 320003, Israel
[2]Department of Electrical and Computer Engineering, University of New Mexico, Albuquerque, New Mexico 87131-0001, USA

[a)]Author to whom correspondence should be addressed: leopoldjg@physics.technion.ac.il

ABSTRACT

When a magnetized annular relativistic electron beam propagating in a conducting tube carries a charge higher than the space charge limit, it can stabilize at a lower energy and higher density state. Such a charge distribution can be used as an electron source in high power microwave devices, a relativistic magnetron in particular, and in other applications. The limiting current transmitted by the beam decreases in tubes with larger radii, so in a tube with a radial transition from a small to large radius, the current can over-inject the downstream tube. This can start a dynamical process which stabilizes as a high density state. The same effect can be achieved by increasing the magnetic field in a magnetic mirror-like scheme or by adding a slowing down potential in the electron beam's route. Here, we propose a simpler, more practical way to produce such a dense state by splitting the cathode into an emitter and a reflector. This scheme is tested in simulation and experiment.

I. INTRODUCTION

The limiting current, I_{LC}, of a strongly magnetized rigid relativistic annular electron beam of radius r_b propagating in a conducting tube of radius R was evaluated by Brejzman and Ryutov[1] and is dependent on the ratio of the tube-to-beam radii and the electron's energy as:

$$I_{LC} = 17\left(\gamma^{2/3} - 1\right)^{3/2} \Big/ \left[2\ln\left(\frac{R}{r_b}\right)\right] [\mathrm{kA}], \tag{1}$$

where $\gamma = 1 + \frac{eV}{mc^2}$ is the relativistic factor, eV is the energy of electrons, m the electron mass, c the speed of light, and 17 kA is the Alfvén current. A correction introduced by Fedosov[2] to Eq. (1), when the presence of the cathode and the width of the beam are considered, is given as:

$$I_{LC} = 17\times(\gamma - \gamma_F)\left(\gamma_F^2 - 1\right)^{\frac{1}{2}}/[2\gamma_F \ln(R/r_b)]\,[\mathrm{kA}], \tag{2}$$

where $\gamma_F = (2\gamma + \frac{1}{4})^{1/2} - \frac{1}{2}$.

For a tube consisting of sections of various radii, the limiting current I_{LC} is determined in the tube with the largest radius. An injected current I_{inj} from an upstream electron source exceeding the limiting current, $I_{inj} > I_{LC}$, leads to the formation of a virtual cathode (VC) in this section and a return current from the VC toward the electron source. These reflected electrons form a sufficiently large negative space charge near the electron source to decrease the emitted current. The space charge of these circulating electrons accumulates in the entire space between the source and the VC, an unstable situation which relaxes to a state of high density and low energy electrons which was named a *squeezed state* by Ignatov and Tarakanov.[3] Such systems were extensively studied over the last 50 years, mainly in the former USSR,[4–8] since it was thought that a squeezed state is an ideal electron source to be used in high power microwave (HPM) devices. A squeezed state was first demonstrated experimentally by Belomyttsev *et al.*[9] and the emission properties of magnetically insulated coaxial diodes within this context have been studied recently in detail.[10]

Recently, Fuks *et al.*[11] have demonstrated that by manipulating the tube radii, an extended VC and a squeezed state are formed, which can be used as the electron source in a magnetron with diffraction output (MDO). This is an advantageous scheme for a relativistic magnetron since there is no magnetron cathode involved, which emits electrons from the boundary of the explosive plasma formed on its surface. This plasma is known to expand across the cathode–anode gap, which becomes smaller while changing the magnetron properties and eventually when the plasma reaches the anode block, pulse shortening occurs.[12]

Instead of anode radius manipulation, Gromov *et al.*[13] suggested that a squeezed state can be obtained in a uniform anode tube by a mirror-like magnetic field, which reduces the electron beam radius.

For an adiabatic increase in the axial component of the magnetic field from B_1 to B_2, the annular beam radius decreases from r_{b1} to r_{b2} as[13]

$$r_{b2} = r_{b1}\left(\frac{B_1}{B_2}\right)^{1/2}. \quad (3)$$

The decrease in the electron radius increases the density of the electron space charge, decreasing the value of I_{LC} so that a return current and an extended VC form, just like when the electron beam encounters an increase in tube radius. Following this idea, Fuks and Schamiloglu[14] suggested and demonstrated by simulation the application of such a magnetic field distribution in an MDO with improved efficiency. It should be noted that earlier, Dubinov[15] had considered the concept of a magnetic mirror to increase the charge contained in a vircator oscillator.

Leopold *et al.*[16] have shown that overcharging a region of the beam propagation can also be enhanced by adding an external second slowing down potential. The latter is difficult to realize for voltages above a few tens of kV, whereas the scheme based on increased magnetic field requires the addition of a second very high magnetic field, both difficult to implement in practice. Siman-Tov *et al.*[17] have replaced the proposed slowing down potential with a partially transparent reflector attached to the cathode using a central conducting rod. The reflector, the rod, and the cathode acquire almost the same potential. This is essentially a beam slowing down scheme, which increases the charge in the gap between the emitter and the reflector, and since the reflector is transparent, excess charge is also released as small electron bunches. These bunches then interact resonantly with the adjacent cavity inducing electromagnetic fields, which in turn modulate the electron beam causing the growth of huge current oscillations fed by the charge trapped in the emitter–reflector gap, refilled as long as the cathode emits electrons. We proposed this method to avoid squeezing (charge accumulation and relaxation) and rather get the accumulated charge to oscillate. This scheme has been tested experimentally[17] to obtain a train of periodic electron beam bunches.

In the present paper, we study the split cathode with a non-transparent reflector and show that when the reflector is opaque the dynamics is different from when it is transparent, similar to the magnetic mirror scheme but more practical. We present MAGIC[18] PIC simulations demonstrating the formation of a low energy high density electron cloud which can be used as a virtual cathode in a magnetron. An experiment to confirm this scheme is also presented.

In all our 3D MAGIC PIC simulations, we used a varying mesh (0.1–0.5 mm cells), with a time step chosen to be half of the 3D Courant limit corresponding to the smallest mesh size. The number of macro-particles in each run was of the order of $2–5 \times 10^6$. Convergence tests were performed to test the adequacy of our choice of spatial resolution and the number of emitted particles at each time step. No particles other than electrons were considered.

II. PRODUCING A LOW ENERGY, HIGH DENSITY STATE USING A SPLIT CATHODE

The idea of a split cathode has been presented in Ref. 17. A split cathode configuration is displayed in Fig. 1, where a PIC simulated electron beam flowing between the emitter and an opaque reflector held together using a central rod is seen 6 ns after a voltage of 450 kV rising in 1 ns has been applied between the cathode and the grounded anode tube. A static uniformly distributed axial magnetic field of 4 T strongly magnetizes the beam. In this simulation, the dimensions and the applied voltage have been chosen to be the same as those of the model studied in Ref. 13 and the reflector attached to the cathode with the rod replaces the role of the magnetic field increase, which in Ref. 13 was from 4 to 12 T.

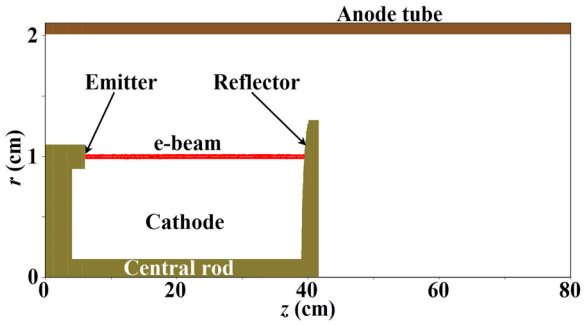

FIG. 1. A cross section of the axially symmetric arrangement of a split cathode made up of an emitter, a reflector, and a central rod placed coaxially inside an anode tube. The beam snapshot is at 6 ns for an applied voltage of 450 kV.

To compare the two systems, we have also modeled the increasing magnetic field by an arrangement of solenoids that produces a magnetic field which on-axis has a profile as shown in Fig. 2. This profile is almost the same everywhere in the 2 cm radius cylindrical volume and is fixed in time.

The axial magnetic field shown in Fig. 2 is almost constant up to z ~30 cm, where it rises from 4 T to ~12 T. The electron beam is affected by the rise in the magnetic field and, as expected [Eq. (3)], its radius reduces as seen in Fig. 3 for the same voltage and at the same time as shown in Fig. 1.

The decrease in the beam radius as shown in Fig. 3 changes the limiting current [Eq. (3)], and a return current develops. This is similar to the slowing down of the beam near the reflector, which increases the space charge locally. The dynamics of this process is seen in Fig. 4, where the $[z,V_z]$ phase space for both cases is compared. The return current develops for the reflector case much earlier [Fig. 4(a)] than for the magnetic mirror case [Fig. 4(b)]. The system then stabilizes around a phase space island between the two VCs for both cases [Figs. 4(c) and (d)]. For the magnetic mirror case [Fig. 4(d)] at the downstream VC, some excess current continues to flow downstream to the walls. With the reflector [Fig. 4(c)], some current is collected on it but the

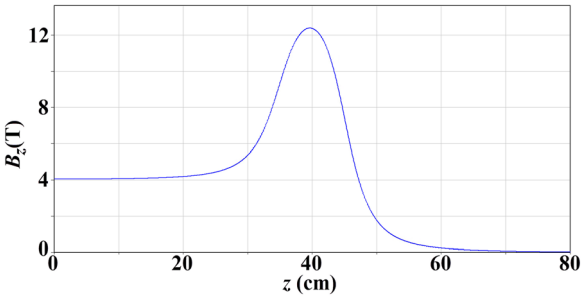

FIG. 2. The axial magnetic field used with a regular cathode.

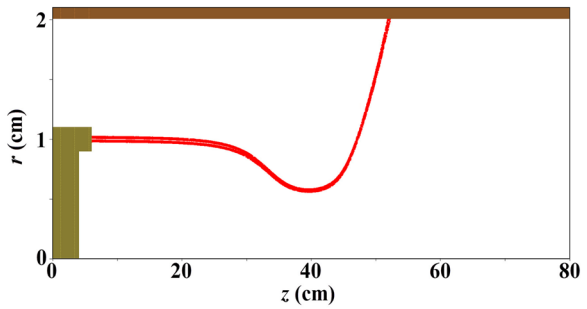

FIG. 3. The electron beam snapshot for a cylindrical cathode immersed in the magnetic field shown in Fig. 2 and otherwise the same conditions and time as shown in Fig. 1.

majority of electrons are reflected and some current flows upstream from the emitter. The $[z,V_r]$ phase space for the two cases at the same time as that shown in Figs. 4(c) and (d) is seen in Figs. 4(e) and (f), respectively. The charge density distributions at the same time as shown in Figs. 4(c) and (d) are seen in Figs. 4(e) and (f), respectively, for the two compared cases.

In Fig. 5, we compare the longitudinal distribution of the electron density [Fig. 5(a)] and the average kinetic energy distribution along the axis [Fig. 5(b)] at a time when the dynamics has stabilized for both configurations. The two cases are similar with a small advantage to the reflector. The electron current flowing upstream from the emitter toward the upstream boundary seen in Figs. 4(c) and (d) is negligible. The current collected on the anode for the magnetic mirror scheme is the same as the current everywhere in the system and the beam reaches the anode at the energy supplied by the applied voltage. The current collected on the reflector is small and the electrons reach the collector with negligible energy [Fig. 5(b)].

We have demonstrated that a split cathode produces a low energy dense electron cloud just like a magnetic mirror. A radial transition in the outer tube or a sudden magnetic field increase can be replaced by a split cathode which is simpler and more practical.

III. EXPERIMENTAL SETUP

In this section, we report the results of an experiment in which the production of a state with high charge density and low energy electrons by the split cathode method is verified. The experiment, the setup of which is seen in Fig. 6, is performed in a 124 mm diameter stainless steel tube in the center of which a 40 mm diameter, 62 mm long anode insert made of stainless steel is placed. Around the tube, a solenoid has been wound which provides a uniform ∼1 T axial magnetic field pulse with a half-period of 15 ms. The solenoid is energized by a 1.1 kA amplitude current pulse produced by the discharge of a 4 mF capacitor preliminarily charged to 1.3 kV using a triggered vacuum spark gap. The pulsed power source used in the experiments was a Marx generator[19] which consists of 12 pulse forming network stages, each of ∼7 Ω impedance and a pulse duration of ∼250 ns. When a matched resistive load of ∼84 Ω is attached, the amplitude of the generator's high voltage (HV) output pulse was ∼140 kV and ∼200 kV, for a charging voltage of 25 kV and 35 kV, respectively. In the experiment, the HV pulse is applied on 20 cylindrical hollow emitters (each 5 mm long and 1.5 mm/0.75 mm in outer/inner diameter) consisting of carbon capillaries attached to the circular perimeter of a hollow aluminum cathode of 16 mm-diameter (see Fig. 6). Earlier studies showed that these types of emitters have low threshold voltages (<15 kV/cm) for plasma formation and electron beam generation of several kA/cm^2 current densities.[20,21] The cathode had an outer diameter of 25 mm to prevent backward flow of electrons and was coated with an 80 μm-thick Al_2O_3 ceramic layer to protect it from possible explosive emission because of plasma formation on its surface.[22] The axial distance between the edge of the capillaries and the anode insert was 20 mm. The reflector was a 2 mm-thick, 40 mm-diameter aluminum disk with a 6 mm diameter ring attached at its periphery to decrease the disk's edge electric fields. The reflector was connected to the cathode center using a 5 mm diameter aluminum central rod (see Fig. 6). The reflector and the central rod were also coated by an 80 μm-thick Al_2O_3 ceramic layer (Fig. 7). The distance between the reflector and the anode radial transition was 40 mm. A small 1 mm hole in the reflector disk at the radius of the annular beam is used to probe the electron current collected on the reflector.

The waveforms of the voltage applied to the diode and the total current were measured using a resistive voltage divider (VD) and a self-integrating Rogowski coil, respectively. The resistive VD was connected to the output of the Marx generator. The Rogowski coil was located at the entrance to the anode tube in the large vacuum chamber (RC in Fig. 6). The magnetic field decreases upstream of this Rogowski coil, which measures the current flowing in the cathode holder and any electron current flowing upstream from the cathode toward the walls of the large vacuum chamber. The electron beam current was measured using a Faraday cup (FC) with a resistive load of either 0.1 Ω (in experiments without the reflector) or 50 Ω (in experiments with the reflector). The distance between the FC and the reflector or in the absence of the reflector, from the anode insert, is 70 mm. A 6 mm diameter hole was drilled in the middle of the anode insert surface. A capacitive VD placed near the surface of the anode insert is connected through this hole to a low-inductance 1.5 kΩ resistor, used to increase its RC time constant to 1.5 μs, connected in series with a 50 Ω load input resistor of the digitizing oscilloscope. This anode VD measures the beam potential and was calibrated accordingly as a resistive VD in shots, in which the length of the cathode holder was increased so that the cathode was downstream from the anode insert. The voltage and current waveforms were acquired using a digitizing DSO80604B oscilloscope (6 GHz bandwidth and 40 GS/s sampling rate). A vacuum of 10^{-3} Pa was kept in the system using turbo-molecular and scroll pumps.

IV. EXPERIMENTAL RESULTS AND COMPARISONS TO SIMULATIONS

In this section, we simulate using the MAGIC PIC code the experimental system of Figs. 6 and 7 without the large diameter upstream vacuum chamber as seen in Fig. 6. We modeled the 20 cylindrical emitters using an annular ring at the radius where the emitters are placed, but the width and the length of the emitters were increased by 2 mm in each open direction to account for the expanding plasma formed by explosive emission. From the surface of this larger annular ring, the current is emitted using a space-charge-limited emission model.

In Fig. 8, we compare the behavior of the system with and without the reflector at $t = 200$ ns. We apply a voltage rising in 40 ns to ∼170 kV and ∼205 kV without and with the reflector, respectively,

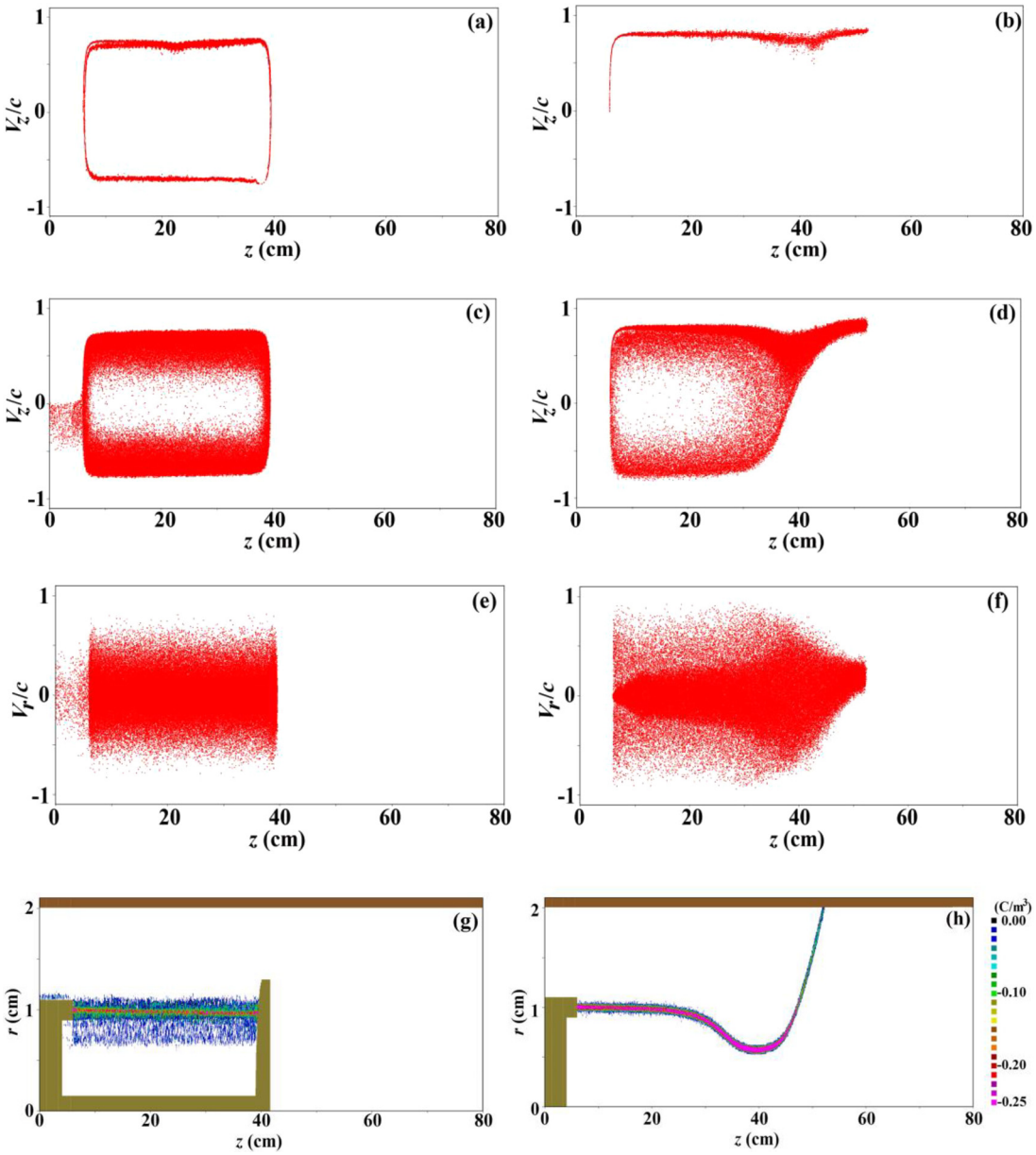

FIG. 4. [z, V_z] phase space for the reflector [(a) at 6 ns and (c) at 45 ns] and for the magnetic mirror [(b) at 6 ns and (d) at 45 ns] cases. [z,V_r] phase space for the reflector (e) and the magnetic mirror (f) cases at 45 ns. Electron charge density distribution at 45 ns for the reflector (g) and the magnetic mirror (h) cases [the color bar is the same for (g) and (h)].

typical to the experiments. In Fig. 8(a), the current as a function of the axial dimension is drawn for the two cases. Without the reflector, a steady current flows from the emitter to the FC. The reflector reflects the electron flow and there are both downstream (negative) and upstream (positive) currents shown in Fig. 8(a), with a small net downstream current reaching the reflector and a small upstream current (∼4–10 A) flowing upstream above the cathode radius. Without the reflector, the average electron energy increases as the beam departs from the emitter, reducing in the larger radius section downstream from the anode insert and finally accelerating to the FC [see Fig. 8(b)]. With the reflector, the energy of both downstream (positive) and upstream (negative) flows is much smaller than the applied voltage; the electrons slow down near the emitter and the reflector, and the small current upstream from the cathode reaches a relatively high energy [see Fig. 8(b) and compare with Fig. 5(b)].

In Fig. 8(c), we compare the longitudinal electron density distribution which behaves in a similar way as shown in Fig. 5(a); that is, between the cathode and the reflector, the longitudinal density is

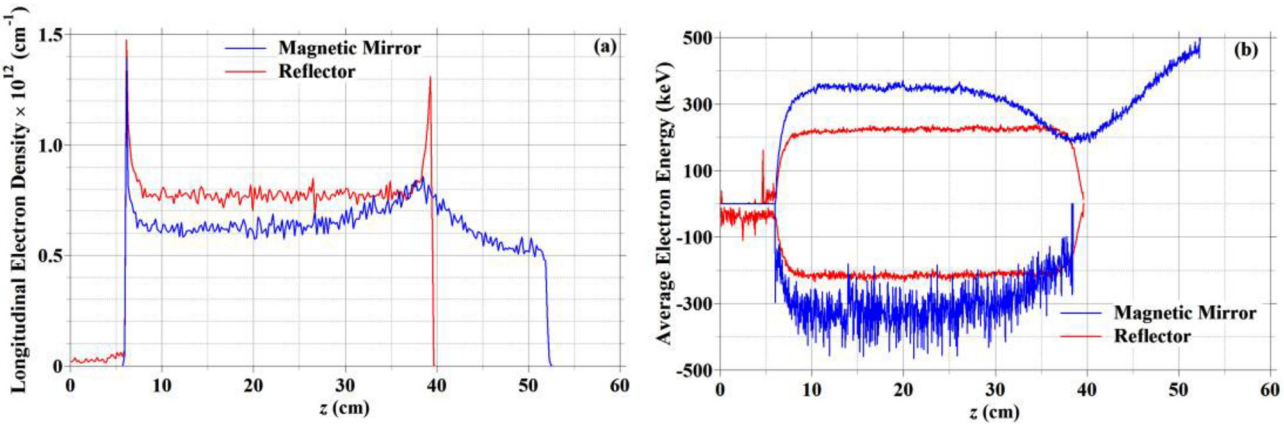

FIG. 5. The longitudinal electron density measured in $\Delta z = 2$ mm bins (a) and the average electron kinetic energy (positive and negative for downstream and upstream flowing electrons, respectively) (b) vs z for the magnetic mirror (red) and reflector (blue) cases at 45 ns.

much higher than in the absence of the reflector. Figure 8(d) shows the kinetic energy distribution of the electrons in the volume bounded by the anode insert for the two cases. This distribution is peaked at a considerably lower energy when the reflector is present. Finally, in Fig. 8(e), we present the electron charge contained in the same volume as shown in Fig. 8(d) as a function of time. During the 250 ns considered, in the presence of the reflector, the charge becomes considerably larger and it seems that there is even space for more low energy charge.

These simulation results confirm that, by using the split cathode in the experimental configuration, a low energy, high density electron charge accumulates in the space between the cathode and the reflector. In the experiment, though, most of the parameters shown in Fig. 8 cannot be measured directly. Note that when the reflector is present, no current flows to the anode.

In Fig. 9, we present comparisons of the voltage and the current in the experiment and in the simulations. The applied voltage is measured in the experiment by the VD placed in the generator oil tank [Fig. 9, (12) and (13)], whereas the current including any return current is measured [Fig. 9, (22) and (23)], by the Rogowski coil (RC) placed at the downstream edge of the large vacuum chamber (see Fig. 6). The voltage [Fig. 9, (11) and (14)] and current [Fig. 9, (21) and (24)] are measured in the simulations in the upstream section of the small vacuum tube along the cathode holder. The maximum of the voltage in the simulations was chosen to be close to the experimental

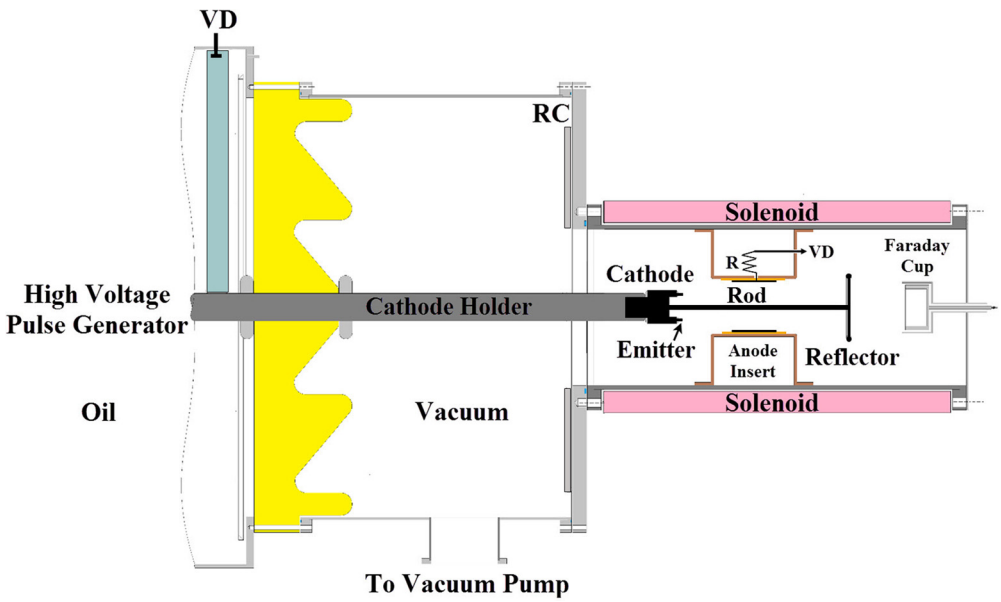

FIG. 6. The experimental setup. The split cathode (Fig. 7) consisting of the cathode, the reflector, and the rod is colored black and is placed along the axis of the anode insert.

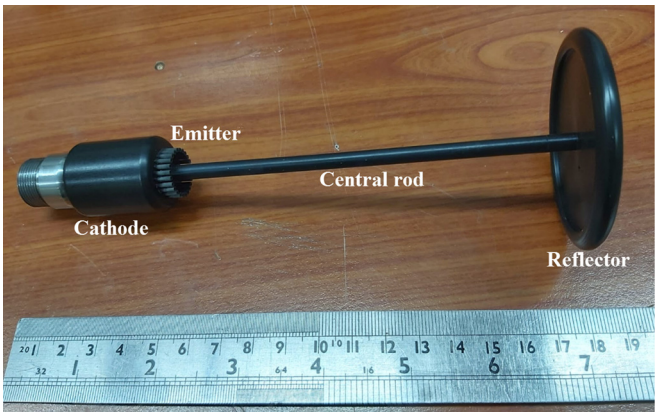

FIG. 7. Photograph of the hard anodized cathode, the emitter, and the attached rod and reflector. This split cathode device appears in Fig. 6 and is modeled in the PIC simulations in Sec. IV.

value. Without the reflector, the total current reaches a value of ∼500 A and the calculated value is close to that measured in the experiment. When the reflector is present, no current flows to the anode [Fig. 9 (24)]. The experimental current trace in Fig. 9 (23) rises first to a value of ∼100 A and decreases toward zero during the rise time of the voltage. This is mostly the effect of the displacement current due to parasitic capacitance, which we estimate to be ∼10 pF. When the voltage reaches its peak value, the total current oscillates around zero within $\sim\pm 200$ A ($t \leq 100$ ns) and then it becomes nearly zero. Note that the simulated value also oscillates around zero current, but between $\sim\pm 40$ A. The experimental enhancement up to ∼100 ns is probably the result of a resonant interaction of the charge oscillations in the cathode–reflector gap with the upstream cavity not included in the simulations (see Ref. 17). The frequency of these oscillations is ∼350 MHz, both in the simulation and the experiment. For a single electron to make a round trip between the emitter and the reflector (24.8 cm) in a period corresponding to this frequency, its energy should be ∼25 keV. In Fig. 8(b), the calculated average energy for this case is ∼50 keV, but in Fig. 8(d), we see that most electrons are ∼10 keV electrons; therefore, it is reasonable to relate the observed frequency to transit time oscillations between the emitter and the reflector which is close to the eigenfrequency of the upstream cavity.[17]

Figures 10(a) and (b) display the time-dependent voltage measured by the capacitive VD placed at the center of the anode insert (see the VD in Fig. 6) without and with the reflector, respectively. When no reflector is present, the VD measures a voltage difference between the anode wall and the axis of ~ -40 kV. With the reflector present, this value increases to ~ -200 kV up to ∼120 ns. The simulated voltage differences for the two cases are very close to these values [Fig. 10(c)]. At ∼125 ns, the measured voltage starts to increase to very large values and drops to zero at ∼225 ns. When the rod holding the reflector (2.5 mm radius) is present, the voltage difference between the anode wall and the rod is almost equal to the applied voltage. In Fig. 10(d), we see that by 125 ns, the electron cloud has expanded almost to the anode wall and that the return current flows upstream above the cathode. We believe that this is the reason for the increased voltage measured by the VD shown in Fig. 10(b), which in the experiment ends in a short-circuit because of the breakdown along the surface of the VD insulator. In the absence of the reflector, the beam does not expand and there is no return current [see Fig. 8(a)]. To summarize, the VD measurement indicates the significant increase in the space charge of electrons in the space beneath the anode insert.

Finally, Fig. 11 shows the current crossing the reflector through a 1 mm diameter hole drilled in it at a radius equal to the emitter radius and measured by the FC. This measurement is an additional indication to the presence of the beam in the space between the emitter and the reflector. The actual values are very small and in Fig. 11 we have multiplied it by assuming that the ratio of beam area and the area of the hole is 350.

Note that the experimental and simulated signals shown in Fig. 11 differ until ∼80 ns. This could be because the beam area expands in time from the emitter radius toward the anode insert radius. The simulated value includes the entire beam, but the sampling hole in the reflector is at a fixed radius and may miss part of the beam at early times. The frequency of the oscillations seen in the PIC calculated current collected on the reflector is again ∼350 MHz and the comparison shown in Fig. 11 with the sample current crossing the hole is quite good.

V. DISCUSSION AND SUMMARY

The experimental and numerical results presented in this paper can be interpreted as follows. In the absence of the electron beam, the potential distributions in the systems without and with a reflector are shown in Figs. 12(a) and (b), respectively. The corresponding potential distributions along the line $r = r_e$, where r_e is the emitter radius, are shown in Fig. 12(c). Magnetized electrons move along the thin-walled tube at radius r_e.

In the presence of the reflector, a single emitted electron oscillates in the potential well with kinetic energy below the applied anode–cathode potential difference. In fact, a single electron energy cannot exceed ∼100 keV [Fig. 12(c)], which agrees with the result of the numerical simulation shown in Fig. 8(d). If the self-consistent space charge electric field of the beam, fluctuating in time, is taken into account, the electron energy can increase or decrease. Electrons with enhanced energy leave the system (absorbed by the cathode or the reflector), while electrons which lose their energy accumulate in the potential well. Thus, the potential well gradually fills with trapped low-energy electrons and its depth decreases. Consequently, new emitted electrons acquire smaller kinetic energy than those emitted earlier and the average energy decreases in time as seen in numerical simulations [see Fig. 8(d)]. Electron accumulation terminates when particles leak from the well due to radial expansion of the electron cloud in a finite magnetic field and electron absorption by the cathode and reflector [Fig. 10(d)].

The term *squeezed state* introduced in Ref. 3 and used in many of the quoted references refers usually to the situation when the area of the phase space island [i.e., Figs. 4(c) and (d)] becomes close to zero. In most practical situations, *squeezing* is only *partial*, though on average, the state of the electron cloud trapped between a VC or a reflector and a cathode is at considerably lower energy and higher density (Fig. 8).

We have shown that a cathode, split into an electron space-charge-limited emitter and a reflector connected using a central

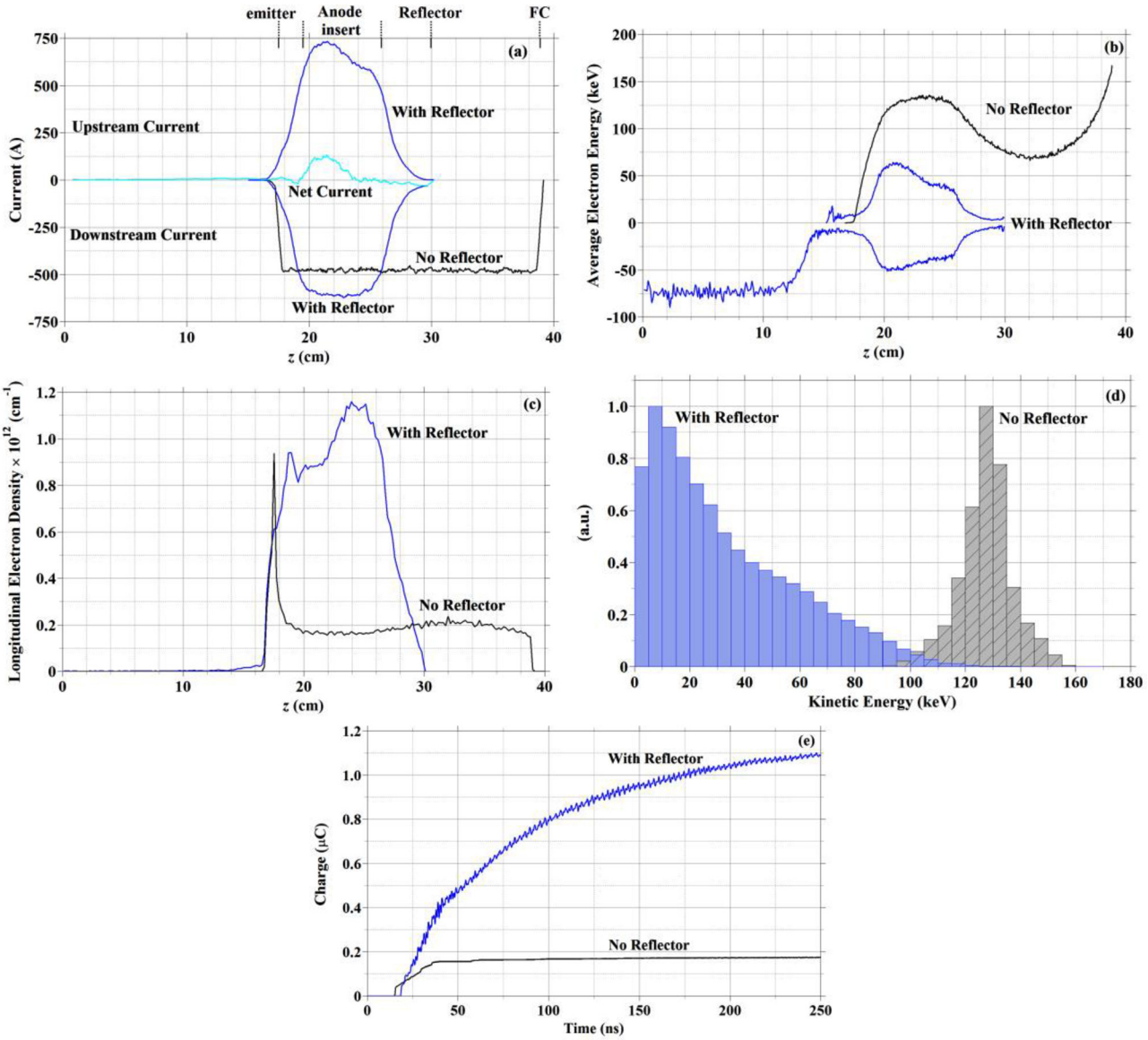

FIG. 8. Comparison of dynamical parameters obtained by PIC simulations at 200 ns with and without the reflector for the experimental system. (a) The downstream (negative) and upstream (positive) currents vs *z*. (b) The downstream (positive) and upstream (negative) average kinetic energy vs *z* with and without the reflector. (c) The longitudinal electron density vs *z*. (d) The kinetic energy distribution in the volume contained by the anode inset normalized to 1 for each case separately. (e) The electron charge vs time in the same volume as shown in (d).

rod, is an effective technique to contain a magnetized partially squeezed electron cloud of low energy and high charge. In fact, a split cathode is a very simple device which can replace the idea of the more complicated magnetic mirror configuration,[13,14] which has been proposed as an advantageous electron source for a relativistic magnetron. The split cathode configuration does not leak current to the walls by design, whereas it is possible that very large magnetic fields would be needed for a magnetic mirror to reflect the entire current. The electrons of the leakage current are accelerated to the walls while acquiring the full energy corresponding to the applied voltage, whereas the electrons collected on the reflector are only slightly above the edge of the potential well mentioned above. The dynamics of the split cathode has been investigated by PIC simulations and the results were confirmed by experiment. The split cathode scheme is an effective means to study the process producing a partially squeezed electron charge and we plan to study this further in future analytical work, simulations, and experiments.

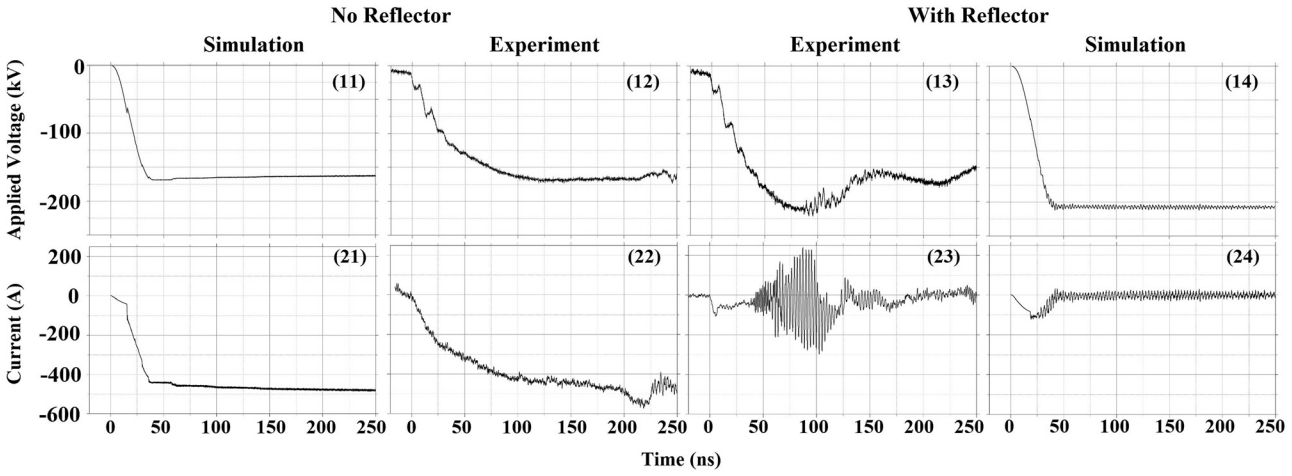

FIG. 9. A matrix of results comparing the experiment to simulations. The applied voltage and the current are drawn in rows 1 and 2. Columns 1 and 2 and columns 3 and 4 are for the cases without and with a reflector, respectively. Columns 2 and 3 are the experimental results. Columns 1 and 4 are the results of simulations.

The MAGIC PIC simulations consider only electron dynamics and do not include the temporal evolution of the cathode explosive emission plasma serving as the source of electrons emitted from its boundary and accelerated toward the anode. We estimate that the plasma travels a few mm downstream along z and a few tenths of mm along r during the few hundred ns of the applied voltage pulse.[24] This affects the value of the emitted current, the conditions for the VC formation in the space between the cathode

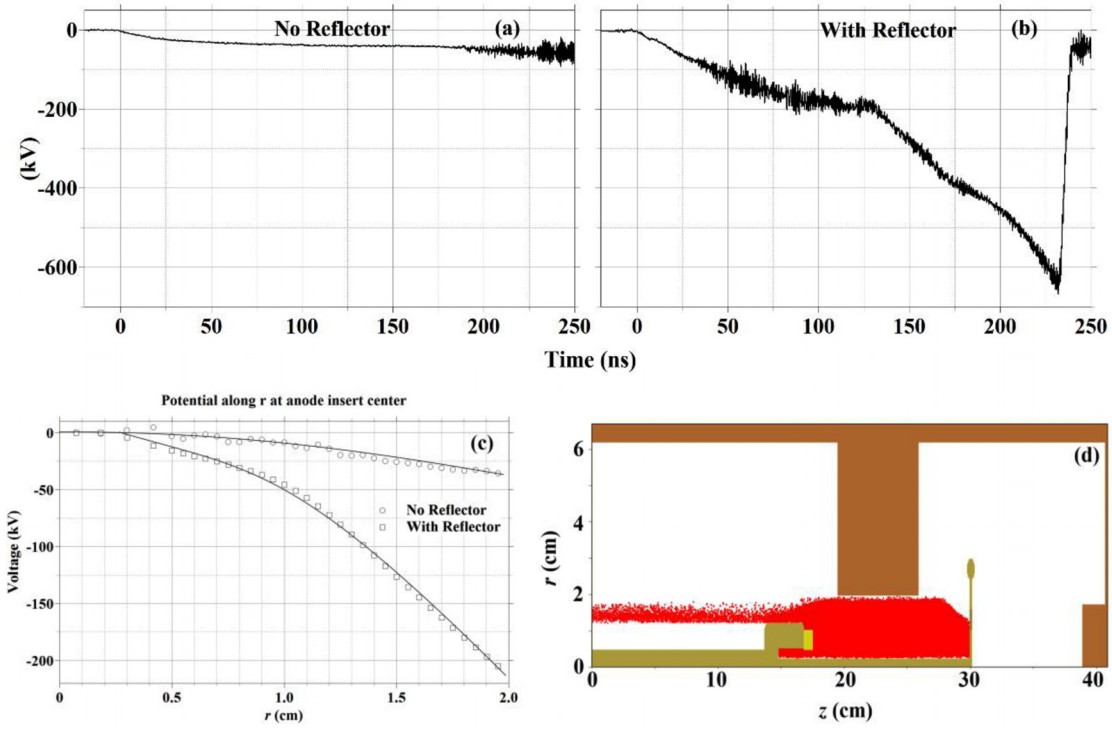

FIG. 10. The voltage vs time measured by the VD placed at the center of the anode inset without (a) and with (b) the reflector. (c) The voltage vs r at the same position calculated by the PIC simulation. The presented values are averaged in time over 10 ns around $t = 200$ ns. (d) The positions of the PIC simulated electron macro-particles in a slice of the configuration space $[z,r]$ at $t = 125$ ns in the presence of the central rod and the reflector modeled after Figs. 6 and 7.

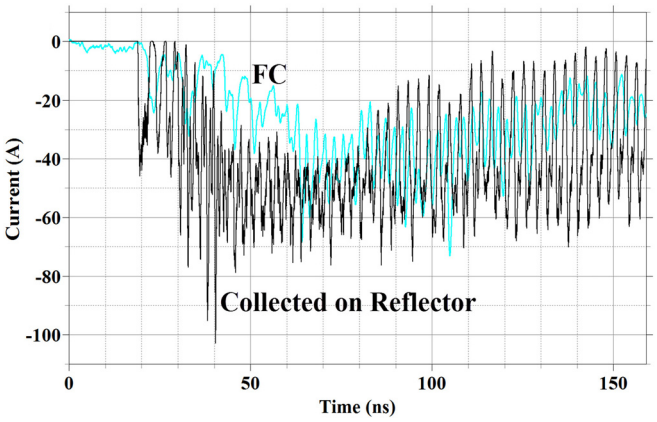

FIG. 11. The current crossing the hole in the reflector and measured by the FC (turquoise curve denoted by the FC) and the PIC calculated current collected on the reflector (black).

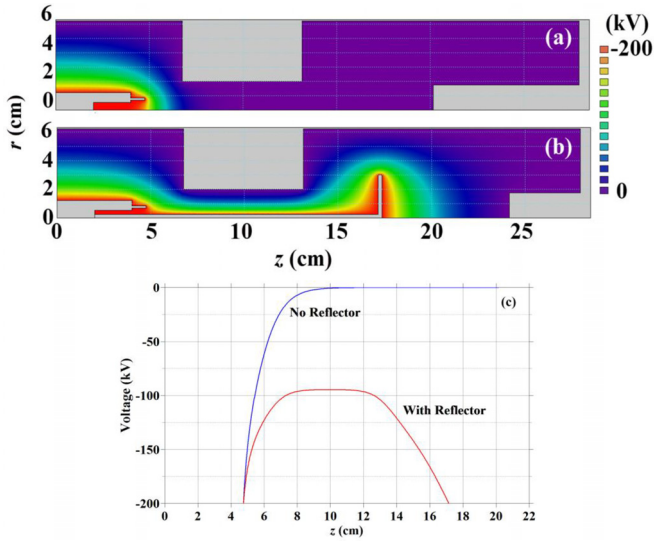

FIG. 12. Equipotential contours[23] in the system without (a) and with (b) a reflector and the potential distributions along the electron beam trajectory at $r = r_e$ (c).

and the reflector, and the matching with the pulse generator. The effect of the plasma's temporal and spatial evolution is not negligible and will be considered in the planning of our future simulations and experiments.

ACKNOWLEDGMENTS

The research at the Technion was supported by Technion Defense Grant No. 2029541 and at the University of New Mexico by AFOSR Grant No. FA9550-19-1-0225 and ONR Grant No. N00014-19-1-2155. The Technion group could not have performed the experiments without the assistance of S. Gleizer and E. Flyat.

DATA AVAILABILITY

The data that support the findings of this study are available from the corresponding author upon reasonable request.

REFERENCES

[1]B. N. Brejzman and D. D. Ryutov, Nucl. Fusion **14**, 873 (1974).
[2]A. I. Fedosov, E. A. Litvinov, S. Y. Belomytsev, and S. P. Bugaev, Sov. Phys. J. **20**, 1367 (1977).
[3]A. M. Ignatov and V. P. Tarakanov, Phys. Plasmas **1**, 741 (1994).
[4]N. F. Kovalev, Tech. Phys. **47**, 906 (2002).
[5]S. Y. Belomyttsev, A. A. Grishkov, S. D. Korovin, and V. V. Ryzhov, Tech. Phys. Lett. **29**, 666 (2003).
[6]A. A. Grishkov, S. Y. Belomyttsev, S. D. Korovin, and V. V. Ryzhov, Tech. Phys. Lett. **29**, 944 (2003).
[7]A. E. Dubinov and I. A. Efimova, Tech. Phys. **46**, 723 (2001).
[8]A. E. Dubinov, A. G. Petrik, S. A. Kurkin, N. S. Frolov, A. E. Koronovskii, and A. E. Hramov, Phys. Plasmas **24**, 073102 (2017).
[9]S. Y. Belomyttsev, A. A. Grishkov, S. A. Kitsanov, S. D. Korovin, S. D. Polevin, V. V. Ryzhov, and A. P. Yachnyi, Tech. Phys. Lett. **31**, 982 (2005).
[10]S. Y. Belomyttsev, V. V. Rostov, I. V. Romanchenko, S. A. Shunailov, M. D. Kolomiets, G. A. Mesyats, K. A. Sharypov, V. G. Shpak, M. R. Ulmaskulov, and M. I. Yalandin, J. Appl. Phys. **119**, 023304 (2016).
[11]M. I. Fuks, S. Prasad, and E. Schamiloglu, IEEE Trans. Plasma Sci. **44**, 1298 (2016).
[12]J. Benford and G. Benford, IEEE Trans. Plasma Sci. **25**, 311 (1997).
[13]A. V. Gromov, M. B. Goykhman, N. F. Kovalev, A. V. Palitsin, M. I. Fuks, and E. Schamiloglu, Tech. Phys. Lett. **44**, 949 (2018).
[14]M. I. Fuks and E. Schamiloglu, Phys. Rev. Lett. **122**, 224801 (2019).
[15]A. E. Dubinov, J. Commun. Technol. Electron. **45**, 792 (2000).
[16]J. G. Leopold, Y. P. Bliokh, M. Siman-Tov, and Y. E. Krasik, Phys. Plasmas **26**, 093107 (2019).
[17]M. Siman-Tov, J. G. Leopold, Y. P. Bliokh, and Y. E. Krasik, Phys. Plasmas **27**, 083103 (2020).
[18]B. Goplen, L. Ludeking, D. Smith, and D. Warren, Comput. Phys. Commun. **87**, 54 (1995).
[19]Y. E. Krasik, A. Dunaevsky, A. Krokhmal, J. Felsteiner, A. V. Gunin, I. V. Pegel, and S. D. Korovin, J. Appl. Phys. **89**, 2379 (2001).
[20]J. Z. Gleizer, T. Queller, Y. Bliokh, S. Yatom, V. Vekselman, Y. E. Krasik, and V. Bernshtam, J. Appl. Phys. **112**, 023303 (2012).
[21]T. Queller, J. Z. Gleizer, and Y. E. Krasik, J. Appl. Phys. **114**, 123303 (2013).
[22]T. Queller, A. Shlapakovski, and Y. E. Krasik, J. Appl. Phys. **108**, 103302 (2010).
[23]S. Humphries, Jr., *Field Solutions on Computers* (CRC Press, 1997).
[24]S. P. Bugaev, V. I. Kanavez, V. I. Koshelev, and V. A. Cherepanov, *Relativistic Multi Wave Microwave Generators* (Siberian Division, Novosibirsk, Nauka, 1991), pp. 81–94 (in Russian).